Low-Power ASK Detector for Low Modulation Indexes and Rail-to-Rail Input Range

Vincenzo Fiore, *Student Member, IEEE*, Egidio Ragonese, *Senior Member, IEEE*, and Giuseppe Palmisano, *Senior Member, IEEE*

***Abstract*—A high-performance ultrahigh-frequency amplitude shift keying (ASK) detector for low-power radio-frequency (RF) receivers is proposed. The circuit is based on a high-gain common-source topology with a feedback loop that provides adaptive biasing. Hence, high sensitivity and rail-to-rail input operation are achieved along with low power consumption. The detector was implemented in a standard 130-nm complementary metal–oxide–semiconductor technology. Sensitivity measurements demonstrate correct detection of a 2-Mb/s ASK-modulated 915-MHz signal with a peak level and a modulation index of around 200 mV and 5%, respectively, which means an envelope signal amplitude of as low as 5 mV. The circuit draws less than 3.4 μA from a 1.2-V power supply while operating with rail-to-rail RF variations and modulation indexes from 5% to 100%. This performance makes the detector suitable for batteryless systems with RF energy harvesting.**

***Index Terms*—Amplitude shift keying (ASK) demodulator, ASK receiver, batteryless radio-frequency (RF) system, complementary metal–oxide–semiconductor technology, envelope detector, low power consumption, RF harvester, ultrahigh-frequency integrated circuit.**

I. Introduction

AMPLITUDE Shift Keying (ASK) is the most common modulation technique for low-power radio-frequency (RF) applications due to its very simple coding and detection circuits. It is defined by the modulation index h, namely, $1 - A_{\rm MIN}/A_{\rm MAX}$, being $A_{\rm MIN}$ and $A_{\rm MAX}$ the minimum and maximum amplitudes of the RF carrier, respectively. The typical architecture of an ASK receiver is shown in Fig. 1(a). It is usually composed of an RF amplifier with automatic gain control, an ASK detector, and a decoder. The ASK detector is the key building block of the receiver. Its main figure of merit is the sensitivity that is the minimum envelope amplitude at which it can be operated. It depends on both h and the amplitude of the RF signal. Although several ASK systems adopt high h values, there are applications for short-range communication, such as RF identification tags [1], [2] or, more generally, batteryless systems with RF energy harvesting, where a low modulation index is important to increase the average input power of the harvester and hence the operating distance for a fixed peak power. Another key issue of batteryless systems is that the envelope detector has to operate with a large RF input range due to the variable operating distance. Finally, a low h also reduces out-of-band interferers. The power consumption for these applications is typically in the microwatt range [1], [2].

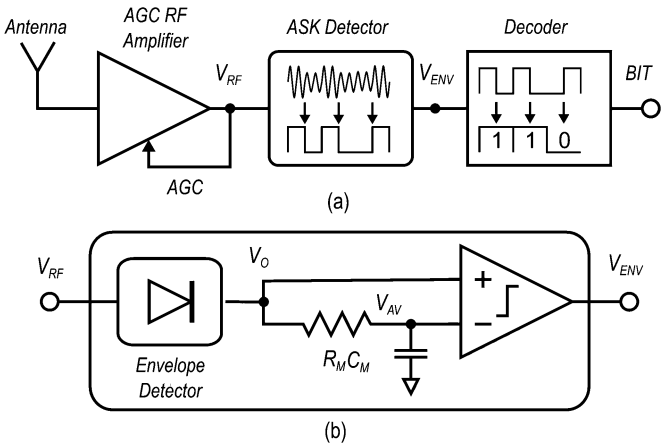

Fig. 1. Typical architecture of (a) an ASK receiver and (b) an ASK detector.

The most commonly used ASK detection approach is shown in Fig. 1(b). The envelope detector (ED) delivers an output voltage, i.e., V_O, whose main signal component is proportional to the envelope signal of the RF input, i.e., $V_{\rm RF}$. The low-pass filter, i.e., $R_M C_M$, provides the comparator with the reference voltage $V_{\rm AV}$ that is the average value of V_O. A rail-to-rail signal, i.e., $V_{\rm ENV}$, is achieved at the comparator output. The sensitivity of the detector depends on the ED sensitivity and the comparator resolution. The ED can be implemented with passive or active topologies. A passive ED [1], [2] does not require a bias current but suffers from low input impedance that is also greatly dependent on the input power. Moreover, it exhibits a transfer loss that reduces sensitivity. An active ED can instead be implemented by exploiting the nonlinearity of the metal–oxide–semiconductor (MOS) transistor in the well-known configuration stages, i.e., common-drain (CD) [3], [4], common-gate (CG) [5], [6], and common-source (CS) [7]–[10]. Differently from passive EDs, the active topologies usually draw a bias current from the power supply. Among the active topologies, the CD detector is the most widely used since it exhibits simplicity, high input impedance, and low current consumption. However, its conversion gain is lower than one, thus affecting the detector sensitivity and the power consumption of the comparator. On the other hand, the CG

Manuscript received April 13, 2015; revised September 4, 2015; accepted November 21, 2015. Date of publication November 25, 2015; date of current version April 28, 2016. This brief was recommended by Associate Editor M. Onabajo.

V. Fiore was with the Dipartimento di Ingegneria Elettrica, Elettronica e Informatica (DIEEI), Università di Catania, 95125 Catania, Italy. He is now with DICE GmbH & Co KG, 4040 Linz, Austria (e-mail: vfiore@dieei.unict.it).

E. Ragonese is with STMicroelectronics, 95121 Catania, Italy (e-mail: egidio.ragonese@st.com).

G. Palmisano is with the Dipartimento di Ingegneria Elettrica, Elettronica e Informatica (DIEEI), Università di Catania, 95125 Catania, Italy (e-mail: giuseppe.palmisano@dieei.unict.it).

Digital Object Identifier 10.1109/TCSII.2015.2503651

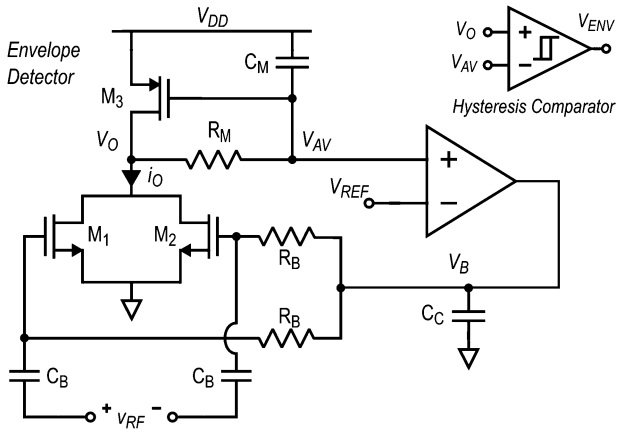

Fig. 2. Proposed ASK detector.

detector has the potential for high gain but shows low input impedance that could impact power consumption. The most interesting topology for high sensitivity and low power consumption is the CS configuration that provides high input impedance and high gain. Unfortunately, the few published examples of CS ED do not provide a solution capable of operating with low h and large RF input ranges [7]–[10]. Indeed, CS EDs suffer from an average current greatly varying with the RF signal that gives envelope distortion, high power consumption, and saturation.

In this brief, a novel CS ASK detector with an adaptive bias approach is proposed. Different from previous published works, the circuit provides high sensitivity and low power consumption while operating with low modulation indexes and rail-to-rail input ranges. This performance well satisfies the requirements of batteryless transceivers with RF energy harvesting.

II. Circuit Description

The schematic of the detector is shown in Fig. 2. The circuit is made up of an ED, which includes a feedback loop with an error amplifier, and a hysteresis comparator. The differential RF input, i.e., $V_{\rm RF}$, is ac-coupled to the detector by means of a high-pass filter, i.e., R_BC_B. The output current, i.e., i_O, of the input pair, i.e., M_{1-2}, flows into a self-biased load that is formed by transistor M_3 and the low-pass filter, i.e., R_MC_M. The feedback loop, including the ED and the error amplifier, sets voltage $V_{\rm AV}$ to the value of reference voltage $V_{\rm REF}$ and defines accordingly the RF input bias voltage V_B. $V_{\rm AV}$ is the average component of output voltage V_O. The feedback loop does not affect the envelope signal transfer since the loop bandwidth is set much lower than the envelope frequency.

When an ASK-modulated RF signal is applied, the input pair produces a rectified output current that will flow into the self-biased load and provides output voltage V_O, as discussed below. Voltage V_O and its average value $V_{\rm AV}$ are fed to a hysteresis comparator [11] that produces a rail-to-rail version of the envelope signal at its output. A diode-connected p-type MOS transistor and a reference current generator are used to set $V_{\rm REF}$ and to perform a pseudo current mirror with M_3. This bias approach provides control of the average current in $M_{1,2}$ and hence accuracy against process, voltage, and temperature (PVT) variations. Moreover, it sets the common-mode input voltage for the hysteresis comparator.

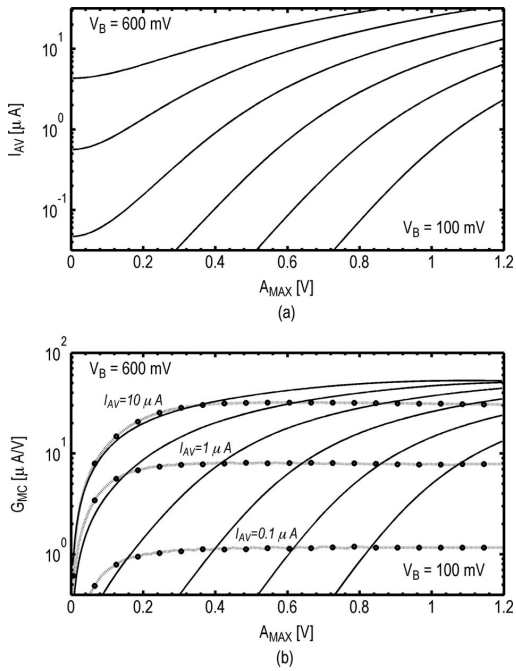

Fig. 3. (a) Simulated $I_{\rm AV}$ and (b) $G_{\rm MC}$ of the input pair versus $A_{\rm MAX}$ and for $V_{\rm B}$ varying from 100 to 600 mV with a 100-mV step.

A. Analysis of the ED

To better understand the circuit operation and highlight the critical aspects of the CS stage of the ED, the behavior of the input pair, i.e., M_{1-2}, is analyzed when an RF input signal is applied and for a fixed bias voltage V_B (i.e., the feedback loop is not active). Due to the nonlinearity of the input pair, output current i_O shows an average component, an envelope signal, and RF harmonics. Neglecting RF terms, for an input signal with a small modulation index, output current i_O in a first-order approximation can be written as

$$i_O = I_{\rm AV} + G_{\rm MC} \times v_{\rm ENV} \tag{1}$$

where $I_{\rm AV}$ is the output average current, $G_{\rm MC}$ is the conversion transconductance gain of the input pair, and $v_{\rm ENV}$ is the envelope input voltage. Let us now consider the current-to-voltage conversion at the output of the input pair. The RF spurious components of i_O will be largely filtered out by the parasitic capacitance at the drain of M_{1-3}, and current $I_{\rm AV}$ will flow into transistor M_3, thus producing average voltage $V_{\rm AV}$. Due to the low-pass filter, i.e., R_MC_M, whose cutoff frequency is set much lower than the envelope frequency, the envelope signal current will flow into resistance R_M and will give output voltage V_O. The conversion voltage gain, i.e., A_C, is then

$$A_C = G_{\rm MC} \times R_M. \tag{2}$$

Fig. 3(a) and (b) shows average current $I_{\rm AV}$ and transconductance gain $G_{\rm MC}$, respectively, for the input pair $M_{1,2}$ versus the peak amplitude of the RF signal, i.e., $A_{\rm MAX}$. $G_{\rm MC}$ was evaluated by setting h as low as 5%. Six curves are shown with voltage V_B ranging from 100 to 600 mV. The aspect ratios listed in Table I were used. Fig. 3(b) also shows $G_{\rm MC}$ for three values of $I_{\rm AV}$, which were kept constant by properly setting V_B according to the value of $A_{\rm MAX}$. Fig. 3(a)

TABLE I
DESIGN PARAMETERS OF THE PROPOSED ASK DETECTOR

$M_{1,2}$	M_3	R_M	R_B	C_M	C_B	C_C	I_A	I_{AV}	I_{COMP}	V_{DD}
[μm/μm]		[MΩ]		[pF]			[μA]			[V]
2/1	1/1	1	0.2	7	0.5	5	0.1	1.75	1.2	1.2

and (b) show that both $I_{\rm AV}$ and $G_{\rm MC}$ greatly vary with $A_{\rm MAX}$ and V_B and that $G_{\rm MC}$ rapidly drops to zero for small RF inputs since the rectifying action of the input pair reduces. However, $G_{\rm MC}$ is almost constant in a large RF input range provided that $I_{\rm AV}$ is kept constant, as demonstrated by the dotted lines in Fig. 3(b), which show $G_{\rm MC}$ for $I_{\rm AV}$ of 0.1 μA, 1 μA, and 10 μA.

In previous published works of CS ED, average current control is not adopted, and hence only envelope detection is possible due to the use of high modulation indexes (usually on–off keying). In fact, the high gain of the CS ED switches the output voltage between the positive and negative output saturation voltage that is imposed by the output swing limitations. However, envelope detection with low h values and large RF signals is not possible with the CS ED without current control. Indeed, the output voltage would be forced by the high gain to the negative saturation level with both $A_{\rm MAX}$ and $A_{\rm MIN}$ RF amplitudes, and the envelope signal would be lost. Accordingly, no solution of high-gain ED (i.e., based on the CS or the CG stage) that is capable of detecting ASK-modulated RF signals with low h and high RF amplitudes exists in the literature. Fig. 3(a) and (b) suggests that, in the presence of large input variations and low values of h, a dynamic adjustment of V_B according to the RF input level should be used to keep constant $I_{\rm AV}$ and, hence, $G_{\rm MC}$. In the proposed circuit, this adaptive bias approach is achieved due to the feedback loop. Indeed, when the RF input signal increases, V_B decreases to maintain almost constant $I_{\rm AV}$, thus producing a constant $G_{\rm MC}$ for small h values. Therefore, the proposed topology allows the high-gain potential of the CS ED to be fully exploited.

B. Adaptive Bias Approach

By inspecting Fig. 2, the small-signal loop gain, i.e., $T(s)$, can be calculated by taking into account the output resistance of the error amplifier $r_{\rm oA}$, its transconductance g_{mA}, and the bias couple capacitor C_B, at the RF input. Due to the low loop bandwidth, resistances R_B can be neglected, and capacitors C_B go in parallel with C_C. A simplified expression of the compensated loop gain is given by

$$T(s) = \frac{g_{mA} r_{oA} g_{m1,2}/g_{m3}}{(1 + s r_{oA}[C_C + 2C_B])\,(1 + sC_M/g_{m3})}. \quad (3)$$

By using a dominant pole approximation, the loop gain–bandwidth product,i.e., $f_{\rm GBW}$, can be evaluated as

$$f_{\rm GBW} = \frac{g_{mA} g_{m1,2}/g_{m3}}{2\pi[C_C + 2C_B]}. \quad (4)$$

$f_{\rm GBW}$ is set much lower than the frequency of the envelope signal, and hence the detector conversion gain is not affected by the feedback loop.

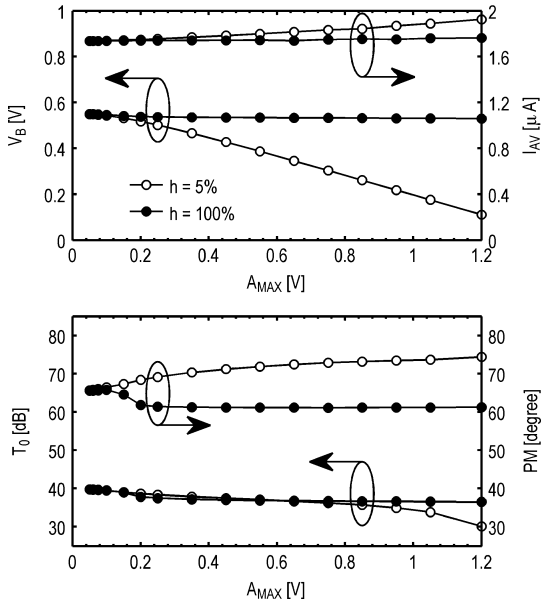

Fig. 4. Simulated V_B, $I_{\rm AV}$, T_0, and PM for h of 5% and 100%.

The error amplifier in the feedback loop is a simple differential amplifier with current-mirror active load whose transistors are biased in subthreshold and draw an overall bias current as low as 100 nA. This way, maximum gain-to-current ratio and low g_{mA} are achieved, which means low power and small compensation capacitor. The loop is stable with a 5-pF compensation capacitor, i.e., C_C, and exhibits a phase margin of about 64° with a 90-kHz $f_{\rm GBW}$. This low value of $f_{\rm GBW}$ guarantees that the loop acts only on average current $I_{\rm AV}$, assuming a target bit rate of 2 Mb/s.

The complete ASK detector was simulated using the design parameters in Table I in which I_A and $I_{\rm COMP}$ are the current consumption of the error amplifier and the comparator, respectively. Specifically, the simulations in Fig. 4 show bias voltage V_B and average current $I_{\rm AV}$ as a function of the maximum amplitude of the modulated RF signal, i.e., $A_{\rm MAX}$, for rail-to-rail input variations and h of 5% and 100%. These curves confirm that, for a large variation of the RF input signal, when h is small the feedback loop produces a large variation of bias voltage V_B, whereas $I_{\rm AV}$ varies only in a small range of values, i.e., from 1.75 μA to 1.95 μA. PVT simulations confirm that $I_{\rm AV}$ changes by less than 2.6% for temperature and power supply variations from −40 °C to 125 °C and ±10%, respectively, across process corners. Moreover, Monte Carlo simulations show that the standard deviation of $I_{\rm AV}$ is 180 nA, which is about 10% of its average value.

Finally, Fig. 4 shows also two main parameters of the feedback loop, i.e., the dc gain T_0 and the phase margin PM. They are always better than 30 dB and 60°, respectively, thus preserving closed-loop accuracy and frequency stability for rail-to-rail input variations.

III. EXPERIMENTAL RESULTS

A micrograph of the detector is shown in Fig. 5. The circuit was fabricated in a $0.13-\mu$m complementary metal–oxide–semiconductor technology provided by STMicroelectronics. The detector area is 87×68 μm^2.

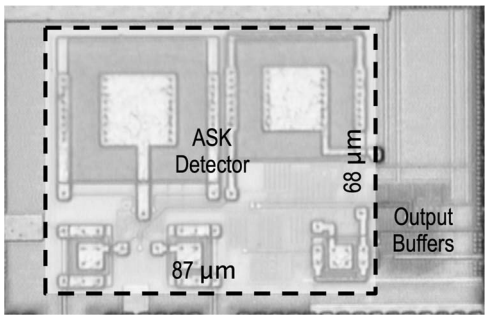

Fig. 5. Micrograph of the ASK detector.

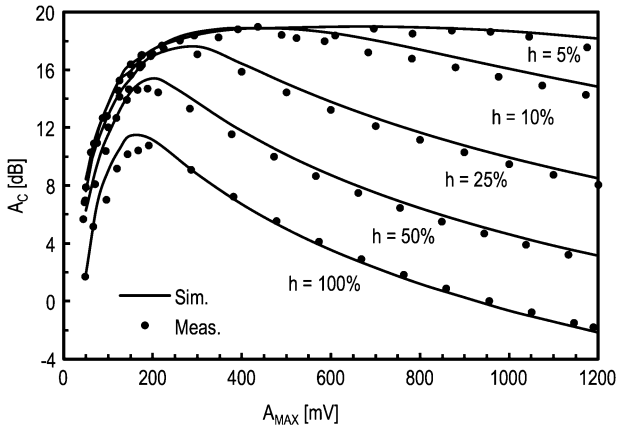

Fig. 6. Measured and simulated conversion gain as a function of A_{MAX}, for various modulation indexes.

The die was wire-bonded to an FR4 printed circuit board using the chip-on-board approach. The 915-MHz input signal drives a 1/4 balun for single-ended-to-differential conversion. It is loaded by a 200-Ω on-board resistor at the secondary coil for impedance matching. The differential signal across the resistor is then applied to the high-impedance input of the detector. On-chip analog and digital buffers were used to measure V_O, V_{AV}, and the comparator output, i.e., V_{ENV}, while avoiding loading effects on the detector. Measurements were performed for a 2-Mb/s ASK square-wave modulated RF input with five different values of h, i.e., 5%, 10%, 25%, 50%, and 100%.

Fig. 6 shows the measured and simulated conversion gain, i.e., A_C, versus the maximum RF amplitude. For h lower than 10%, the gain versus the RF input amplitude is almost constant in a wide range and is around 19 dB. For higher h, the gain decreases with A_{MAX} since the output voltage saturates due to the swing limitation, as previously discussed. In our design, the peak-to-peak output swing is about 800 mV. At low RF inputs, the gain rapidly reduces since linear operation takes place.

The circuit was measured for different h values at the sensitivity condition for the comparator. This condition imposes a peak value of around 32 mV at the comparator input. For h of 5%, 50%, and 100%, the corresponding RF amplitudes are 200, 57, and 52 mV, respectively, and the resulting amplitudes of the input envelope signal (i.e., the ED input sensitivities) are 5, 14.5, and 26 mV, respectively, according to $A_{\mathrm{ENV}} = h/2 \times A_{\mathrm{MAX}}$. The relative gain values for the three envelope signals are 16, 7, and 1.8 dB, respectively. Fig. 7 shows the ED output voltage referred to the average voltage V_{AV} (i.e., $V_O - V_{\mathrm{AV}}$) and the output voltage of the comparator,

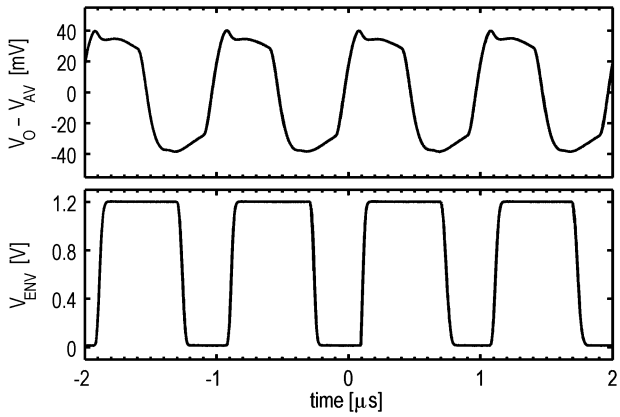

Fig. 7. Measured output waveforms at sensitivity ($h = 5\%$ and $A_{\mathrm{MAX}} = 200$ mV).

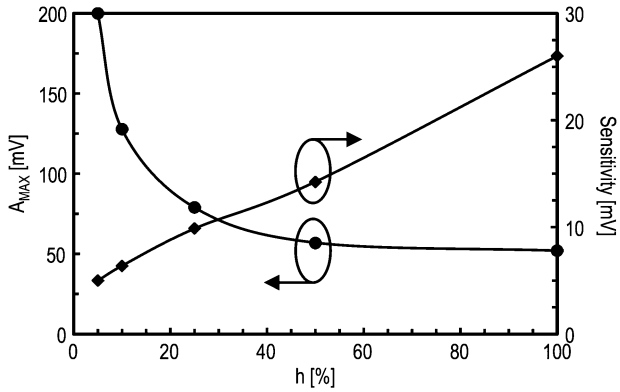

Fig. 8. Measured sensitivity of the proposed detector and corresponding A_{MAX} as a function of modulation index h.

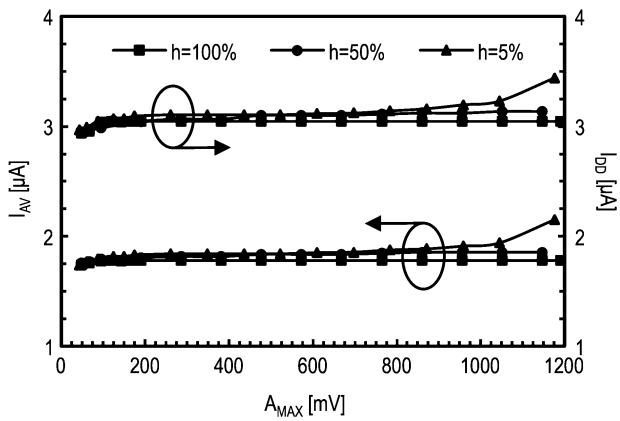

Fig. 9. Measured average current consumption of (a) the input pair (I_{AV}) and (b) the whole ASK detector (I_{DD}) for h values of 5%, 50%, and 100%.

i.e., V_{ENV}, for h of 5% and 200-mV RF amplitude. A more complete measurement of the ED sensitivity and the corresponding RF maximum amplitude, i.e., A_{MAX}, as a function of h is shown in Fig. 8. These two curves show that the best detector sensitivity is achieved with low h since the conversion gain is the highest (see also Fig. 6). On the other hand, a high value of h is needed to work with minimum RF amplitude.

Fig. 9 shows the measured average current I_{AV} of the input pair along with the overall power supply current, i.e., I_{DD}, for

TABLE II
COMPARISON WITH STATE-OF-THE-ART ASK DETECTORS

Name	[2]	[4]	[5]	[6]	[8]	[12]	This work
Topology	Passive	CD	CG	CG	CS	CS	CS
RF frequency	860-960 MHz	1.9 GHz	2.4 GHz	5.8 GHz	20 GHz	40-960 MHz	915 MHz
Bit rate	160 kbit/s	20 kbit/s	5 Mbit/s	14 kbit/s	1.65 Gbit/s	5-6.7 kbit/s	2 Mbit/s
Gain @ 200 mV	-	–6.9 dB	–4 dB	-	–12 dB	-	16 dB (h = 5%) 10.8 dB (h = 100%)
Mod. Index h	80%	100%	100%	85%	100%	100%	> 5%
Input Range	0.25-1.25 V	60-200 mV	25-200 mV	-	10-600 mV	23-56 mV	0.05-1.2 V
Power consumption	0.36 µW	0.2 µW	3 µW	45 µW	> 1.26 mW	5.8–76 nW	< 4.13 µW
Energy/bit	2.25 pJ	10 pJ	0.6 pJ	3.2 nJ	0.76 pJ	1.1-11 pJ	< 2.06 pJ
Technology	0.13 µm	0.13 µm	90 nm	0.13 µm	90 nm	0.18 µm	0.13 µm
Area	-	-	0.018 mm^2	-	-	< 0.170 mm^2	0.006 mm^2

three values of h, namely, 5%, 50%, and 100%. Current $I_{\rm AV}$ is almost constant with the RF amplitude up to 1.2 V, changing only from $1.78\ \mu$A to $2.14\ \mu$A. Moreover, current consumption $I_{\rm DD}$ is almost constant and has an average value of $3.1\ \mu$A in the whole operating range, being the maximum value around $3.44\ \mu$A for the 5% modulated signal. The low dependence of $I_{\rm AV}$ on $A_{\rm RF}$ proves the effectiveness of the feedback loop.

A comparison with the most representative ASK detectors from recent literature is shown in Table II. To the best of our knowledge, the proposed work is the only detector able to operate with an h value of as low as 5% while exhibiting the highest peak-to-peak RF input range. Moreover, the circuit provides the highest gain for both low and high modulation indexes.

Indeed, the gain at 200-mV RF input is 16 and 10.8 dB for h values of 5% and 100%, respectively. As far as the energy per bit is concerned, the proposed detector shows an outstanding value of around 2 pJ in the whole input range that is better than that of the implementations in [4] and [6]. The detectors in [5] and [8] exhibit better values of energy per bit, but they do not include the consumption of the baseband amplification stages that can be even higher than that of the ED if the detector output signal is quite low as in [5] and [8].

On the other hand, the energy per bit reported in [12] highly depends on the RF input power. Indeed, it is around 1 and 11 pJ for input power levels of -22.5 and -15 dBm, respectively. Finally, the energy per bit of our detector is comparable to the passive solution in [2], which does not account for the power subtracted to the RF harvester.

IV. CONCLUSION

A novel solution for ASK detection has been proposed, which exhibits high sensitivity and rail-to-rail RF input capability while dissipating very low power. For the first time, high sensitivity with both low h and large RF input variations is demonstrated. Indeed, operation at 915 MHz with RF input amplitudes from 50 mV to 1.2 V and modulation indexes from 5% to 100% has been successfully validated. With the same modulation indexes, the measured sensitivity goes from 5 to 26 mV. The current consumption in all the operative conditions is lower than $3.44\ \mu$A, and it is almost constant in the whole RF input range. This performance is achieved due to the use of a high-gain CS topology and an adaptive bias approach implemented with a feedback loop. The circuit can be advantageously adopted in batteryless transceivers based on RF energy harvesting where low modulation index and low power consumption are mandatory to preserve harvester sensitivity and, hence, reading range.

REFERENCES

[1] H. Nakamoto *et al.*, "A passive UHF RF identification CMOS tag IC using ferroelectric RAM in $0.35-\mu$m technology," *IEEE J. Solid-State Circuits*, vol. 42, no. 1, pp. 101–110, Jan. 2007.
[2] G. K. Balachandran and R. E. Barnett, "A passive UHF RFID demodulator with RF overvoltage protection and automatic weighted threshold adjustment," *IEEE Trans. Circuits Syst. I, Reg. Papers*, vol. 57, no. 9, pp. 2291–2300, Sep. 2010.
[3] R. G. Meyer, "Low-power monolithic RF peak detector analysis," *IEEE J. Solid-State Circuits*, vol. 30, no. 1, pp. 65–67, Jan. 1995.
[4] B. Otis and J. Rabaey, *Ultra-Low Power Wireless Technologies for Sensor Networks*. New York, NY, USA: Springer, 2007, pp. 53–59.
[5] B. van Liempd *et al.*, "A 3 μW fully-differential RF envelope detector for ultra-low power receivers," in *Proc. IEEE ISCAS*, May 2012, pp. 1496–1499.
[6] J. Choi, K. Lee, S.-O. Yun, S.-G. Lee, and J. Ko, "An interference-aware 5.8 GHz wake-up radio for ETCS," in *Proc. IEEE Int. Solid-State Circuits Conf. Tech. Dig.*, Feb. 2012, pp. 446–448.
[7] S. B. Sleiman and M. Ismail, "Transceiver parameter detection using a high conversion gain RF amplitude detector," in *Proc. IEEE ISCAS*, May 2010, pp. 2059–2062.
[8] J. Lee, Y. Chen, and Y. Huang, "A low-power low-cost fully-integrated 60-GHz transceiver system with OOK modulation and on-board antenna assembly," *IEEE J. Solid-State Circuits*, vol. 45, no. 2, pp. 264–275, Feb. 2010.
[9] X. Huang, P. Harpe, G. Dolmans, H. de Groot, and J. R. Long, "A 780–950 MHz, $64-146\ \mu$W power-scalable synchronized-switching OOK receiver for wireless event-driven applications," *IEEE J. Solid-State Circuits*, vol. 49, no. 5, pp. 1135–1147, May 2014.
[10] V. Fiore *et al.*, "A 13.56 MHz RFID tag with active envelope detection in an organic complementary TFT technology," in *Proc. IEEE Int. Solid-State Circuits Conf. Tech. Dig.*, Feb. 2014, pp. 492–493.
[11] F. Yuan, "Current regenerative Schmitt triggers with tunable hysteresis," in *Proc. IEEE Int. MWSCAS*, Aug. 2009, pp. 110–113.
[12] C. De Roover and M. S. J. Steyaert, "Energy supply and ULP detection circuits for an RFID localization system in 130 nm CMOS," *IEEE J. Solid-State Circuits*, vol. 45, no. 7, pp. 1273–1285, Jul. 2010.